

# $\beta$ -Hairpin Conformation of Fibrillogenic Peptides: Structure and $\alpha$ - $\beta$ Transition Mechanism Revealed by Molecular Dynamics Simulations

Isabella Daidone,<sup>1</sup> Fabio Simona,<sup>2</sup> Danilo Roccatano,<sup>3</sup> Ricardo A. Broglia,<sup>4</sup> Guido Tiana,<sup>4</sup> Giorgio Colombo,<sup>2\*</sup> and Alfredo Di Nola<sup>1\*</sup>

<sup>1</sup>Department of Chemistry, University of Rome "La Sapienza," Rome, Italy

<sup>2</sup>Istituto di Chimica del Riconoscimento Molecolare, CNR, Milano, Italy

<sup>3</sup>School of Engineering and Science, International University Bremen, Bremen, Germany

<sup>4</sup>Department of Physics, University of Milano, Milano, Italy

**ABSTRACT** Understanding the conformational transitions that trigger the aggregation and amyloidogenesis of otherwise soluble peptides at atomic resolution is of fundamental relevance for the design of effective therapeutic agents against amyloid-related disorders. In the present study the transition from ideal  $\alpha$ -helical to  $\beta$ -hairpin conformations is revealed by long timescale molecular dynamics simulations in explicit water solvent, for two well-known amyloidogenic peptides: the H1 peptide from prion protein and the A $\beta$ (12–28) fragment from the A $\beta$ (1–42) peptide responsible for Alzheimer's disease. The simulations highlight the unfolding of  $\alpha$ -helices, followed by the formation of bent conformations and a final convergence to ordered in register  $\beta$ -hairpin conformations. The  $\beta$ -hairpins observed, despite different sequences, exhibit a common dynamic behavior and the presence of a peculiar pattern of the hydrophobic side-chains, in particular in the region of the turns. These observations hint at a possible common aggregation mechanism for the onset of different amyloid diseases and a common mechanism in the transition to the  $\beta$ -hairpin structures. Furthermore the simulations presented herein evidence the stabilization of the  $\alpha$ -helical conformations induced by the presence of an organic fluorinated cosolvent. The results of MD simulation in 2,2,2-trifluoroethanol (TFE)/water mixture provide further evidence that the peptide coating effect of TFE molecules is responsible for the stabilization of the soluble helical conformation. *Proteins* 2004;57:198–204. © 2004 Wiley-Liss, Inc.

**Key words:** misfolding; prion protein; A $\beta$  peptide; amyloid diseases;  $\alpha$ - $\beta$  conformational transition

## INTRODUCTION

The incorrect folding of globular proteins is the result of amino acid mutation, chemical modification, environmental changes, or other unknown factors. The misfolded proteins are often degraded. In some cases, however, they aggregate and form amyloid fibrils, which are associated with some of the most distressing neurodegenerative

diseases,<sup>1</sup> such as prion and Alzheimer's diseases.<sup>2,3</sup> Many sources of evidence suggest that these diseases are associated with an  $\alpha$  to  $\beta$  conformational transition of part of the protein,<sup>4,5</sup> and that a small fragment of the protein plays a key role as misfolding and aggregation precursor.<sup>6,7</sup>

Prion diseases arise through a post-translational change to the so-called prion protein, PrP, whose NMR structure was first resolved by Riek et al.<sup>8</sup> and is characterized by the accumulation of an abnormal form of the prion protein, PrP<sup>Sc</sup>, in the brain.<sup>9,10</sup> Residues 109–122 (H1 peptide) are considered to be important for the  $\alpha$  to  $\beta$  conformational transition and amyloid formation. According to several sources of experimental evidence, the isolated H1 peptide of the normal cellular prion protein, PrP<sup>C</sup>, adopts in water a  $\beta$ -sheet structure from which amyloid fibrils precipitate,<sup>11,12</sup> is able to induce the  $\alpha$ -helix to  $\beta$ -sheet conformational transition of the isolated 129–141 fragment (H2 peptide)<sup>11</sup> and, as part of the synthetic fragment PrP(90–145), can convert PrP<sup>C</sup> to a PrP<sup>Sc</sup>-like form.<sup>13</sup>

Similarly, Alzheimer's disease is the result of deposition in brain tissues of A $\beta$ (1–42) peptides, a product in the amyloid protein metabolism.<sup>3</sup> Shorter and synthetic fragments of the A $\beta$ -peptide (1–28, 25–35, 10–35, and 12–28) have been studied and characterized, in particular the A $\beta$ (12–28) fragment, which was shown to have behavioral effects in mice,<sup>14,15</sup> and formation of fibril aggregates<sup>16</sup> and toxic effects in vitro.<sup>17</sup>

**Abbreviations:** 3D, three-dimensional; CHC, central hydrophobic core; HB, hydrogen bond; HFIP, 1,1,1,3,3,3-hexafluoropropan-2-ol; MD, molecular dynamics; PDB, Protein Data Bank; SAS, solvent-accessible surface area; SPC, simple point charge; TFE, 2,2,2-trifluoroethanol.

Grant sponsor: European Community Training and Mobility of Researchers Program "Protein (Mis)-Folding". Grant sponsor: Italian National Research Council.

\*Correspondence to: Alfredo Di Nola, Department of Chemistry, University of Rome "La Sapienza," P. le A. Moro 5, Rome 00185 Italy. E-mail: dinola@degas.chem.uniroma1.it

Received 16 December 2003; Accepted 17 March 2004

Published online 22 June 2004 in Wiley InterScience (www.interscience.wiley.com). DOI: 10.1002/prot.20178

In TFE or membrane-mimicking environments, both H1 and A $\beta$ (12–28) fragments were shown to adopt an  $\alpha$ -helical conformation.<sup>5,18</sup>

Unfortunately, the insoluble and massive character of the fibrils rule out the possibility to investigate their structure at atomic resolution with conventional experimental techniques, so that the  $\beta$ -structures of these fragments are not available, and the mechanism of the conformational transition is largely unknown. In such cases, one has little choice but to turn to the use of theoretical approaches.

Several studies using MD simulations on model peptides and aggregates have recently appeared in the literature. Levy et al.<sup>19</sup> observed the helix–coil transition of the slightly different PrP(106–126) peptide performing a set of 34 MD simulations. Klimov and Thirumalai<sup>20</sup> showed via MD simulation that the oligomerization of A $\beta$ (16–22) requires the peptide to undergo a random coil to  $\alpha$ -helix to  $\beta$ -strand transition. Straub et al.<sup>21</sup> used the computation of a variationally optimized dynamical trajectory connecting fixed end points of known structure to speed up the conformational transitions among the different secondary structure motifs. On the aggregation side, Caffish and coworkers,<sup>22</sup> for instance, used a simplified implicit model based on the SAS to describe the main solvent effects, to simulate the aggregation process of the heptapeptide GNNQQNY from the yeast prion protein. Other MD simulations with explicit representations of solvent were run on oligomers of the Alzheimer's peptides. The results indicate that A $\beta$ (16–22) has a preference to aggregate in an extended conformation, forming antiparallel  $\beta$ -sheet structures. Longer fragments, instead, tend to aggregate as  $\beta$ -hairpins.

In the present study, we report, for the first time at atomic resolution, the spontaneous transition to the  $\beta$ -hairpin conformations of the Syrian hamster PrP peptide H1 and of the A $\beta$ (12–28) fragment obtained with long time-scale MD simulations in explicit water. The analysis of the trajectories helps define the common and peculiar pattern of the hydrophobic side-chains in the  $\beta$ -hairpin conformation and the common  $\alpha$  to  $\beta$  conformational transition mechanism of these two peptides, which despite having different sequences give rise to the analogous aggregation phenomena. This unbiased MD approach to study amyloid peptides was also tested by the use of a 30% (v/v) TFE/water mixture model of the solvent to check its ability to reproduce the stabilization of the helical conformation in membrane-mimicking environments, by the TFE coating effect already noted in a previous study.<sup>24</sup>

The convergence of the results is particularly significant; actually the peptide H1 and the A $\beta$ (12–28) fragment, although simulated with the same MD package and force field, were studied independently of each other in two different laboratories.

## METHODS

### MD Simulations Protocol

MD simulations in the NVT ensemble, with fixed bond lengths,<sup>25</sup> were performed with the GROMACS software

package<sup>26</sup> and with the GROMOS96 force field.<sup>27</sup> The force field uses an explicit representation of acidic hydrogens and of hydrogen atoms on aromatic rings. Water was modeled by the SPC model<sup>28</sup> and TFE by the Fioroni et al. model.<sup>29</sup> A twin-range cutoff was used for the calculation of the nonbonded interactions. The short-range cutoff radius was set to 0.8 nm and the long-range cutoff radius to 1.4 nm for both Coulombic and Lennard–Jones interactions. The Berendsen algorithm<sup>30</sup> was used for temperature control. The peptides, in their different starting conformations, were solvated with water or the TFE/water mixture and placed in a periodic truncated octahedron large enough to contain the peptide and  $\approx 1.0$  nm of solvent on all sides. In all the simulations of the H1 peptide, a negative counterion, Cl<sup>−</sup>, was added by replacing a water molecule at the most positive electrical potential to achieve a neutral simulation cell. The side-chains were protonated so as to reproduce a pH of about 7 and the N- and C-terminals were amidated and acetylated, respectively, to reproduce the experimental conditions.<sup>11</sup> For the simulations of the A $\beta$ (12–28) fragment, no counterions needed to be added, since the total charge of the peptide was zero. The protonation of the side-chains and the N- and C-terminals was consistent with the experimental pH = 5 condition used by Jarvet et al.<sup>31</sup> All the simulations, starting from the crystallographic structure, were equilibrated with 100-ps MD runs, with position restraints on the protein to allow relaxation of the solvent molecules. These first equilibration runs were followed by other 50-ps runs without position restraints on the protein. The temperature was gradually increased from 50 K to the chosen temperature for performing short runs of 50 ps each, every 50 K.

### MD Simulations of the H1 Peptide

Different MD simulations in explicit water of the H1 peptide (MKHMAGAAAAGAVV) were carried out:

1. A 450-ns MD simulation at 300 K, starting from an ideal  $\alpha$ -helix solvated with 5133 water molecules.
2. A  $\approx 21$ -ns MD simulation in water at two different temperatures:  $\approx 11$  ns at 360 K followed by  $\approx 11$  ns at 300 K. The starting structure was obtained by a clustering procedure performed on the first 200 ns of the previous simulation. The central structure of the most populated cluster turned out to be the one at 84 ns.
3. A 35-ns MD simulation at 300 K in water, starting from a model configuration provided by low resolution X-ray diffraction data solvated with 6411 water molecules.<sup>12</sup>
4. A 50-ns MD simulation at 300 K, starting from an ideal  $\alpha$ -helix in a mixture of 30% (v/v) TFE/water. Although experimentally HFIP was used as cosolvent, we preferred to perform simulation in TFE, since its smaller size allow a larger computational efficiency. Furthermore, TFE is less effective as secondary structure stabilizer than HFIP used in the experiments, so we expect that the results of our simulations are further validate by this fact.

The PDB coordinates file of the low-resolution X-ray structure were downloaded from [http://www.mad-cow.org/~tom/prion\\_QuatStruc.html](http://www.mad-cow.org/~tom/prion_QuatStruc.html).

### MD Simulations of the A $\beta$ (12–28) Peptide

The A $\beta$ (12–28) fragment (VHHQKLFFFAEDVGSNK) was studied with 5 long-timescale MD simulations:

1. Two 100-ns-long MD simulation in water at 295 K and 320 K (in order to speed up the phase space sampling), respectively, starting from an  $\alpha$ -helical conformation, solvated with 3463 water molecules, taken from the PDB 1IYT.pdb file corresponding to the whole A $\beta$ (1–42) peptide.
2. Two MD simulation in water, 30 ns at 295 K and 20 ns at 320 K, respectively, starting from an extended, all *trans*, conformation. This starting conformation was solvated with 11,712 water molecules. The timespan of these two simulations was shorter than the first two due to the much higher number of solvating water molecules.
3. A 100-ns-long MD simulation in water at 320 K, starting from a conformation representative of the most populated cluster obtained from the statistical clustering of the conformations explored in the 4 simulations described above, which was solvated by 3757 water molecules.
4. A 50-ns-long MD simulation of the same peptide at 300 K, in a TFE/water mixture, starting from the same  $\alpha$ -helical conformation as in item 1.

### Clustering Procedure

Cluster analysis was performed using the Jarvis–Patrick<sup>32</sup> method: A structure is added to a cluster when this structure and a structure in the cluster have each other as neighbors and have at least  $P$  neighbors in common. The neighbors of a structure are the  $M$  closest structures. In our case,  $P$  is 3,  $M$  is 9.

## RESULTS

### $\alpha$ -Helix to $\beta$ -Hairpin Transition of the H1 Peptide

A first simulation was performed at 300 K for 450 ns, starting from an ideal  $\alpha$ -helix. The  $\alpha$ -helix structure was completely lost after  $\approx 10$  ns, and after  $\approx 408$  ns a transition to an ordered  $\beta$ -hairpin structure, stable for the remaining 50 ns, was observed [Fig. 1(a)]. The  $\beta$ -hairpin structure [Fig. 2(a)] was of the type 2:2 with a type II'  $\beta$ -turn sequence of (A113-)G114-A115(-A116), and was characterized by a shift in the  $\beta$ -sheet register of the interstrand HB pattern, with an antiparallel bulge involving G119. Interestingly, the hydrophobic residues, and in particular, alanines A113, A115, and A116 in the turn region, were mostly exposed to the solvent, providing a possible seed for the aggregation process. Furthermore, the hydrophobic SAS monitored in the last stages of the  $\beta$ -hairpin folding process for the hydrophobic residues clearly showed a sharp transition from a state of compact bent conformations with buried hydrophobic side-chains, to the  $\beta$ -hairpin state, with increased water accessibility of

the hydrophobic residues (Fig. 3). The final average SAS value was around 9 nm<sup>2</sup>, slightly lower than the value calculated for the  $\alpha$ -helical starting conformation of 9.4 nm<sup>2</sup>.

To speed up the sampling of the conformational space, a further simulation at higher temperature was performed, starting from a configuration obtained by a cluster analysis of the first 200 ns of the previous simulation. The temperature was initially set to 360 K and after  $\approx 11$  ns quenched to 300 K, when an almost complete  $\beta$ -hairpin structure was observed [Fig. 1(a)]. In the last  $\approx 10$  ns, 2 different  $\beta$ -hairpins with an occurrence of 45% and 25%, respectively, were sampled: a 4:4  $\beta$ -hairpin, with a type VIII  $\beta$ -turn sequence of G114-A115-A116-A117 [Fig. 2(b)], and a 2:2  $\beta$ -hairpin, with the same HB pattern and turn sequence observed in the previously reported simulation at 300 K.

The only available experimental model, obtained by low-resolution X-ray diffraction measurements on fibers,<sup>12</sup> suggested the presence of a  $\beta$ -bend with an intramolecular turn. Using this structure as starting point, we performed a 35-ns-long MD simulation in water [Fig. 1(a)]. After  $\approx 8$  ns, the peptide adopted a very stable 4:4  $\beta$ -hairpin conformation [Fig. 2(b)], with the same HB pattern and  $\beta$ -turn sequence observed in the simulation at variable temperature. The only difference was that the  $\beta$ -turn type was IV instead of VIII.

It has to be pointed out that the two types of  $\beta$ -hairpin observed in the different simulations (4:4 and 2:2) have turn regions surprisingly rich in alanines and a peculiar high-solvent accessibility of the hydrophobic residues, hinting at a reasonable starting point for the aggregation process. A  $\beta$ -hairpin like conformation of the H1 peptide, in the scrapie form of the prion protein, was hypothesized by Prusiner and coworkers<sup>33</sup> and by Daggett and coworkers.<sup>34</sup>

### $\alpha$ -Helix to $\beta$ -Hairpin Transition of the A $\beta$ (12–28) Peptide

The conformational evolution of the A $\beta$ (12–28) peptide was investigated by long-timescale simulations at two different temperatures, namely, 295 K and 320 K, using different starting structures.

Two 100-ns-long simulations at the two above-referenced temperatures were started from the helical conformation. The  $\alpha$ -helix was only marginally stable at both the temperatures, and the peptide showed a high tendency to populate a compact bent conformation [Fig. 1(b)]. This was stabilized by the formation of a salt bridge between K16 and E22 or D23, and by the packing of the side-chains of residues 17–21 (LVFFA), the CHC. V24 also packed on this nascent hydrophobic patch.

Two additional simulations (30 ns at 295 K and 20 ns at 320 K) were started from a completely extended structure to check the convergence to the same family of compact states as described above. In both simulations, the peptide evolved into a compact conformational ensemble, characterized by the same features of the bent structure obtained from the two previously described simulations.

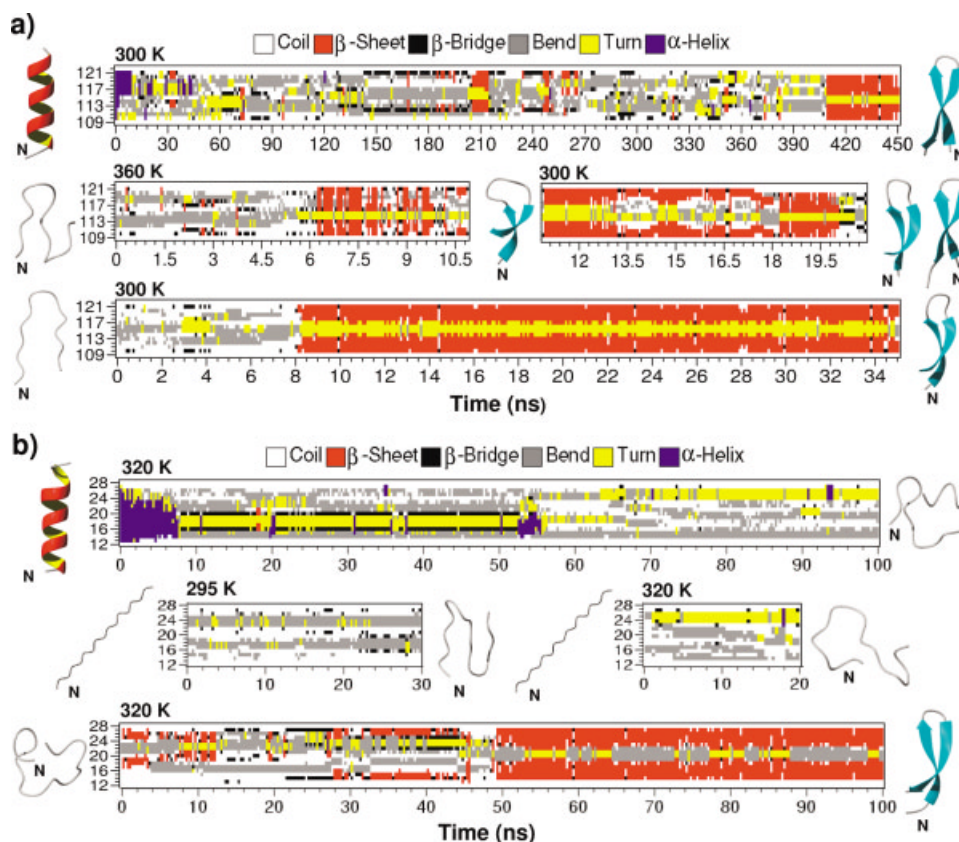


Fig. 1. Time evolution of secondary structure. The analysis was performed with the DSSP program.<sup>42</sup> The starting and final structures of each simulation are shown on the left and right sides, respectively. The N-terminal in each snapshot is indicated with N. (a) Time evolution of the H1 peptide secondary structure. Upper panel: MD simulation at 300 K starting from an ideal  $\alpha$ -helix. Note the formation of the  $\beta$ -hairpin at  $t \approx 408$  ns. Middle panel: MD simulation at variable temperature starting from the central structure of the most populated cluster obtained from the first 200 ns of the previous simulation. Two  $\beta$ -hairpins are formed at  $t \approx 11$  ns and  $t \approx 18$  ns, respectively. Lower panel: MD simulation at 300 K starting from the low resolution X-ray structure. The  $\beta$ -hairpin is formed at  $t \approx 8$  ns. (b) Time evolution of the A $\beta$ (12–28) peptide secondary structure. Upper panel: MD simulation at 320 K starting from an ideal  $\alpha$ -helix. Middle panel: MD simulation at 295 K and at 320 K starting from an extended conformation. Lower panel: MD simulation at 320 K starting from the representative structure of the previous simulations. Note the formation of the  $\beta$ -hairpin at  $t \approx 48$  ns.

A clustering procedure was then applied to the 4 trajectories obtained, and the representative structure of the most populated cluster was isolated and used as a starting point for further MD analysis. This structure, characterized by the presence of a loop comprising residues 22–23 (E–D), and residues 12–21 and 24–28 in extended-bend conformation, was simulated for 100 ns at 320 K. After  $\approx 48$  ns, a sharp transition to a very ordered  $\beta$ -hairpin structure was observed [Fig. 1(b)]. The  $\beta$ -hairpin structure [Fig. 2(c)] was of the type 2:2, with a type II'  $\beta$ -turn sequence of F19–F20–A21–E22.

Very interestingly, the hydrophobic side-chains of LVFFA sequence, as a consequence of being both consecutive in the sequence and in the formation of the turn, were mostly exposed to water and, consistent with the observations in the H1 peptide simulations, an analogue increase in the hydrophobic SAS was observed (Fig. 3) on going from the compact bent conformation to the ordered  $\beta$ -hairpin. The final average SAS value was around  $5.8 \text{ nm}^2$ , lower than the value calculated for the  $\alpha$ -helical starting conforma-

tion of  $8 \text{ nm}^2$ . The final ordered structure of the  $\beta$ -hairpin was consistent with several experimentally based hypotheses on the conformation of the monomer in the fibrils.<sup>7,31,35</sup>

#### $\alpha$ -Helix Stabilization in the TFE/Water Mixture

Conformational studies of both the H1 peptide and A $\beta$ (12–28) fragment have been performed in mixtures of fluorinated solvent and water that were shown to stabilize the helical conformations.<sup>5,18</sup> To investigate this effect and test the simulations against those experimental data, two simulations in  $\approx 30\%$  TFE/water mixture were carried out. In Figure 4, the time percentage of  $\alpha$ -helical conformation per residue for both the simulations is reported. A representative structure of each peptide is also shown. The H1 peptide retains the central core of the initial  $\alpha$ -helix (residues 112–117) during all the simulation time. This result is in excellent agreement with the solid-state NMR data obtained by Heller et al.<sup>18</sup> using the stronger helix stabilizer HFIP, and by Satheeshkumar and Jayakumar<sup>36</sup> on the slightly

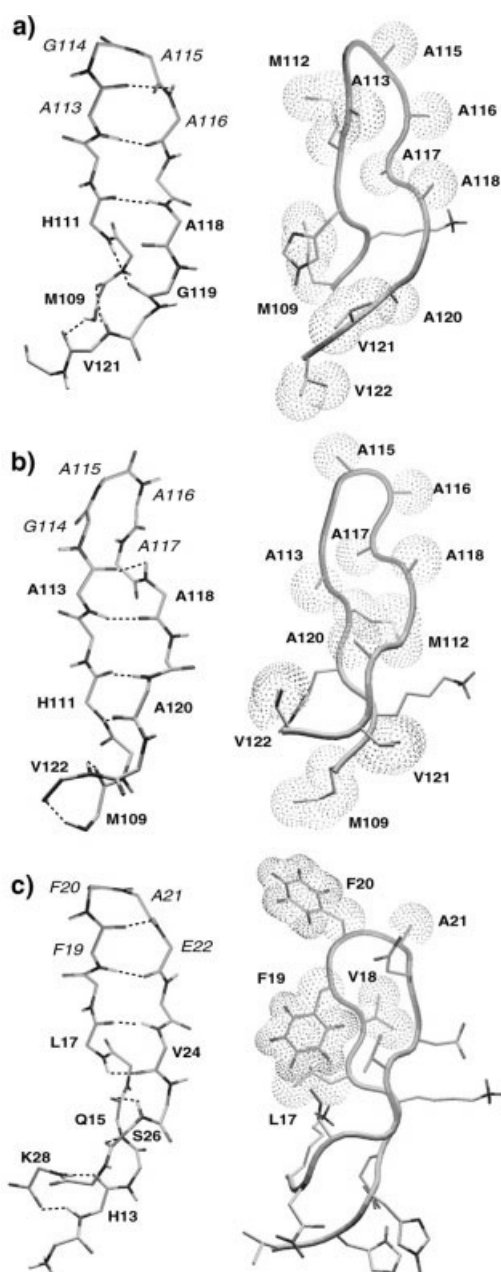


Fig. 2.  $\beta$ -Hairpin structures. (a) Structure of the 2:2  $\beta$ -hairpin, with a type II'  $\beta$ -turn, of the H1 peptide obtained in the 450 ns long MD simulation at 300 K. Note that the alanines, particularly in the turn region (A113, A115, and A116), are exposed to the solvent. (b) Structure of the 4:4  $\beta$ -hairpin, with a type IV  $\beta$ -turn, of the H1 peptide obtained in the 35-ns-long MD simulation at 300 K, starting from the low-resolution X-ray structure. Note that the alanines, particularly in the turn region (A115, A116, and A117), are exposed to the solvent. (c) Structure of the 2:2  $\beta$ -hairpin, with a type II'  $\beta$ -turn, of the  $A\beta(12-28)$  peptide obtained in the 100-ns-long MD simulation at 320 K. Note that the central hydrophobic residues (L17, V18, F19, F20, and A21) are exposed to the solvent. The residues in italics belong to the turn.

different 113–127 peptide. In the case of the  $A\beta(12-28)$  fragment, the helical conformation is retained in regions 13–17 and 21–24, while the central part the structure has the tendency to bend, once more in agreement with the experimental observations.<sup>5</sup>

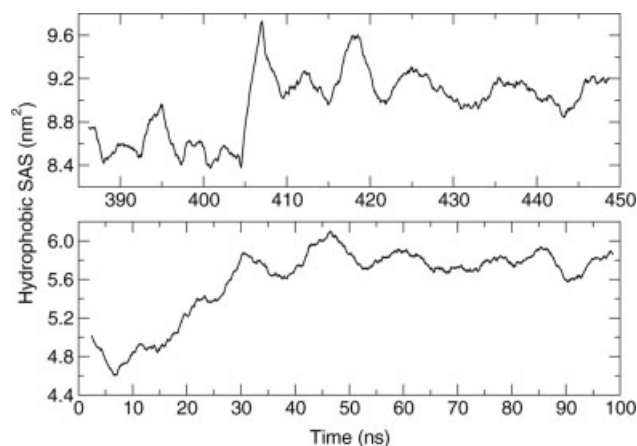


Fig. 3. Hydrophobic SAS as a function of time. **Upper panel:** The SAS variation corresponding to the conformational transition from bent to  $\beta$ -hairpin geometry at 300 K for the H1 peptide. Note the increase of the hydrophobic SAS at  $t \approx 408$  ns, corresponding to the bent to  $\beta$  transition. **Lower panel:**  $\beta$  transition at 320 K of the  $A\beta(12-28)$  peptide in the MD simulation at 320 K. The starting structure in the figure corresponds to the representative structure obtained by a cluster analysis (see text). The maximum hydrophobic SAS is obtained in correspondence of the transition from disordered bent to the ordered  $\beta$ -geometry at  $\approx 48$  ns. For the  $A\beta(12-28)$  peptides, just the central hydrophobic residues are considered. The plots shown are results of box car averaging over a 10-ps window. General features are insensitive to the nature of this averaging.

In a recent MD study of peptide-forming secondary structure in TFE/water mixture,<sup>24</sup> it has been shown that in a TFE/water mixture, the organic cosolvent aggregates around the peptide, forming a matrix that partly excludes water. This process in turn promotes the formation of local interactions and, as a consequence, stabilizes the folded structures.<sup>24,37</sup> A similar coating effect is also the basis of the increased stability of helical conformations in the cases examined herein. The average number of contacts of the TFE molecules with the peptide in the first 200 ps and in the last 5 ns is  $191 \pm 30$  and  $349 \pm 33$  for the H1 peptide, and  $293 \pm 33$  and  $525 \pm 42$  for the  $A\beta(12-28)$  peptide, respectively. In both cases, an increase of  $\approx 85\%$  is observed, showing a clear propensity of TFE to coat the solute, in agreement with the previous observation by Roccatano et al. on Melittin peptide.<sup>24</sup>

## DISCUSSION

Taken together, the results obtained from our totally unbiased simulations indicate an extremely high conformational flexibility for both peptides in water solution, with a general high tendency to form ordered  $\beta$ -sheet structures. The observed  $\beta$ -hairpin conformations are characterized by an increased hydrophobic SAS with respect to the compact bent conformation preceding the transition. In the ordered  $\beta$ -structure, all of the hydrophobic side-chains lie on the same plane around the turn region of the hairpin, and point into the same direction in 3D space. In contrast, in the starting  $\alpha$ -helical conformations of both peptides, the hydrophobic side-chains are “scattered” on different faces of the helix, and as a result of geometrical and sequence constraints, they point in different directions. This is a new feature in  $\beta$ -hairpin conformations, as

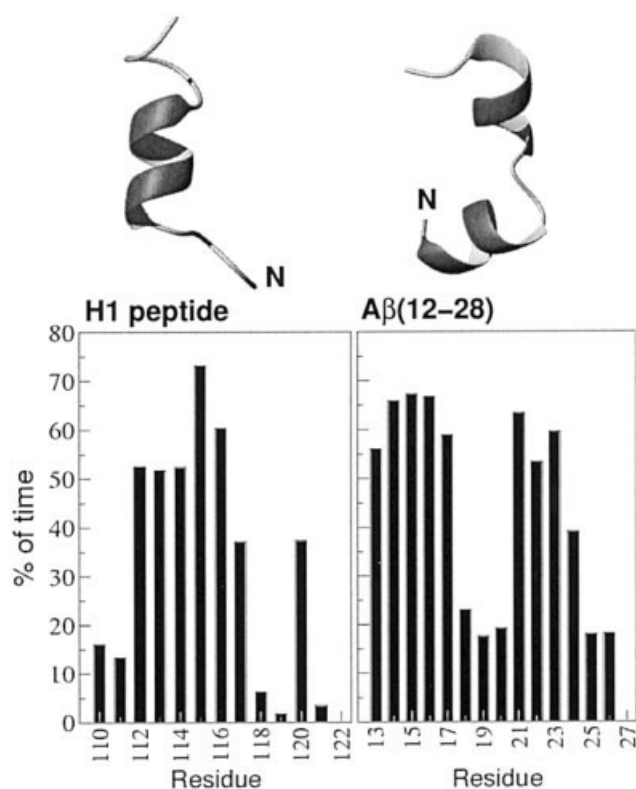


Fig. 4. Time percentage of  $\alpha$ -helical conformation per residue for the H1 peptide (left) and for the A $\beta$ (12–28) peptide (right) in the TFE/water mixture simulations. A representative structure extracted at 50 ns for both peptides is also shown. The N-terminal in each snapshot is indicated with N.

the structures so far obtained for other peptides show large intramolecular hydrophobic interactions,<sup>38</sup> with a clear tendency to remove hydrophobic side-chains from water contact in order to avoid aggregation phenomena. Although the presence of 5 consecutive hydrophobic residues (LVFFA) in A $\beta$  peptide and the unusual hydrophobic patch in H1 is not well represented in protein sequences, analogous highly hydrophobic sequences in  $\alpha$ -helical geometries are also present in some “nonamyloidogenic” proteins known to aggregate in amyloidogenic conditions, such as in the case of lysozyme<sup>39</sup> or myoglobin.<sup>40</sup> Thus, it is conceivable that these very peculiar sequences and the conformational transitions into the  $\beta$ -hairpin geometry conspire to expose part of the hydrophobic cores of the two peptides. These types of structures can be considered as highly frustrated and offer a clear starting point for aggregation. Despite showing a lower or comparable global hydrophobic SAS with respect to the  $\alpha$ -helical conformation, the steric properties and the ordered directionality of the exposed patches in the  $\beta$ -hairpin conformations may define a possible ordered hydrophobic interaction area with other molecules sharing the same structural features. This sort of preorganized interaction area is absent in the helical conformation, and these observations can theoretically support the observation of high percentages of  $\beta$ -structures in experimental studies.<sup>4,6,31,35</sup>

More specific interactions, such as Coulombic interactions, in addition to the hydrophobic collapse, should be considered necessary for the subsequent ordering of the nascent fibrillar aggregates, as shown in the case of experimentally studied small peptide models.<sup>41</sup>

The transition from  $\alpha$ -helical to  $\beta$ -structure requires the peptides to populate intermediate  $\beta$ -bend geometries in which several mainly hydrophobic interactions are partially formed. This is followed by the sudden collapse to ordered  $\beta$ -hairpin structures and the simultaneous disruption of the hydrophobic side-chain interactions, with a consequent increase in the solvent exposure. For both H1 and A $\beta$ (12–28) peptides, the atomic picture of the detailed mechanism of the evolution from  $\alpha$  to  $\beta$  provided in this work can be very useful for the design of new constrained sequences or new drug candidates.

Finally, the simulations in the TFE/water mixture evidence the stability of  $\alpha$ -helical conformations in the presence of the fluorinated cosolvent, resulting in excellent agreement with the available experimental data. Furthermore, the analysis of the TFE distribution around the peptide confirms the mechanism of TFE stabilization proposed by Roccatano et al.<sup>24</sup> on different secondary structure-forming peptides.

## ACKNOWLEDGMENTS

We thank Professors Maurizio Brunori, Giacomo Carrea, and Martin Zacharias for carefully reading the manuscript and for stimulating discussions.

## REFERENCES

- Shastry BS. Neurodegenerative disorders of protein aggregation. *Neurochem Int* 2003;43:1–7.
- Prusiner S. Prions. *Proc Natl Acad Sci USA* 1998;95:13363–13383.
- Selkoe D. Alzheimer's disease: genes, proteins, and therapy. *Physiol Rev* 2001;81:741–766.
- Pan KM, Baldwin M, Nguyen J, Gasset M, Serban A, Groth D, Mehlhorn I, Huang Z, Fletterick RJ, Cohen FE, Prusiner SB. Conversion of  $\alpha$ -helices into  $\beta$ -sheets features in the formation of the scrapie prion proteins. *Proc Natl Acad Sci USA* 1993;90:10962–10966.
- Jayawickrama D, Zink S, Velde DV, Effiong R, Larive C. Conformational analysis of the  $\beta$ -amyloid peptide fragment,  $\beta$ (12–28). *J Biomol Struct Dyn* 1995;13:229–244.
- Peretz D, Williamson R, Matsunaga Y, Serban H, Pinilla C, Bastidas R, Rozenshteyn R, James T, Houghton R, Cohen F, Prusiner S, Burton D. A conformational transition at the N terminus of the prion protein features in formation of the scrapie isoform. *J Mol Biol* 1997;273:614–622.
- Mihara H, Takahashi Y, Ueno A. Design of peptides undergoing self-catalytic  $\alpha$  to  $\beta$  transition and amyloidogenesis. *Biopolymers* 1998;47:83–92.
- Riek R, Hornemann S, Wider G, Billeter M, Glockshuber R, Wuthrich K. NMR structure of the mouse prion protein domain prp(121–321). *Nature* 1996;382:180–182.
- Borchelt DR, Scott M, Taraboulos A, Stahl N, Prusiner SB. Scrapie and cellular prion proteins differ in the kinetics of synthesis and topology in cultured cells. *J Cell Biol* 1990;110:743–752.
- Prusiner S, Scott MR, DeArmond SJ, Cohen FE. Prion protein biology. *Cell* 1998;93:337–348.
- Nguyen J, Baldwin MA, Cohen FE, Prusiner SB. Prion protein peptides induce  $\alpha$ -helix to  $\beta$ -sheet conformational transitions. *Biochemistry* 1995;34:4186–4192.
- Inouye H, Kirschner DA. Polypeptide chain folding in the hydrophobic core of hamster scrapie prion: analysis by X-ray diffraction. *J Struct Biol* 1998;122:247–255.

13. Kaneko K, Peretz D, Pan KM, Blochberger T, Wille H, Gabizon R, Griffith O, Cohen F, Baldwin M, Prusiner S. Prion protein (prp) synthetic peptides induce cellular prp to acquire properties of the scrapie isoform. *Proc Natl Acad Sci USA* 1995;92:11160–11164.
14. Flood JF, Morely JE, Roberts E. Amnestic effects in mice of four synthetic peptide homologous to amyloid  $\beta$ -protein in patients with Alzheimer's disease. *Proc Natl Acad Sci USA* 1991;88:3363–3366.
15. Flood JF, Morely JE, Roberts E. An amyloid  $\beta$ -protein fragment, A $\beta$ -(12–28), equipotently impairs post-training memory processing when injected into different limbic system structures. *Brain Res* 1994;663:271–276.
16. Fraser PE, Nguyen JT, Surewicz WK, Kirschner DA. pH dependent structural transitions of Alzheimer's amyloid peptides. *Biophys J* 1991;60:1190–1201.
17. Fraser PE, Levesque L, McLachlan, DR. Alzheimer's A $\beta$ -amyloid forms an inhibitory neuronal substrate. *J Neurochem* 1994;62:1227–1230.
18. Heller J, Kolbert AC, Larsen R, Ernst M, Bekker T, Baldwin M, Prusiner SB, Pines A, Wemmer DE. Solid-state NMR studies of the prion protein H1 fragment. *Protein Sci* 1996;5:1655–1661.
19. Levy Y, Hanan E, Solomon B, Becker OM. Helix–coil transition of prp106–126: molecular dynamic study. *Proteins* 2001;45:382–396.
20. Klimov DK, Thirumalai D. Dissecting the assembly of A $\beta$ (16–22) amyloid peptides into antiparallel  $\beta$ -sheets. *Structure* 2003;11:295–307.
21. Straub JE, Guevara J, Huo S, Lee JP. Long time dynamic simulations: exploring the folding pathways of an Alzheimer's amyloid A $\beta$  peptide. *Acc Chem Res* 2002;35:473–481.
22. Gsponer J, Habberthuer U, Caflisch A. The role of side chain interactions in the early steps of aggregation: molecular dynamics simulations of an amyloid-forming peptide from yeast prion Sup35. *Proc Natl Acad Sci USA* 2003;100:5154–5159.
23. Ma BY, Nussinov R. Stabilities and conformations of Alzheimer's beta-amyloid peptide oligomers [A beta(16–22), A beta(16–35) and A beta(10–35)]: sequence effects. *Proc Natl Acad Sci USA* 2002;99:14126–14131.
24. Roccatano D, Colombo G, Fioroni M, Mark A. Mechanism by which 2,2,2-trifluoroethanol/water mixtures stabilize secondary-structure formation in peptides: a molecular dynamics study. *Proc Natl Acad Sci USA* 2002;99:12179–12184.
25. Hess B, Bekker H, Berendsen HJC, Fraaije, JGEM. Lincs: a linear constraint solver for molecular simulations. *J Comp Chem* 1997;18:1463–1472.
26. van der Spoel D, van Drunen R, Berendsen HJC. GROningen MAchine for Chemical Simulation. Department of Biophysical Chemistry, BIOSON Research Institute, Nijenborgh 4 NL-9717 AG Groningen; 1994. E-mail: gromacs@chem.rug.nl
27. van Gunsteren WF, Billeter SR, Eising AA, Hünenberger PH, Krüger P, Mark AE, Scott WRP, Tironi IG. Biomolecular simulation: the GROMOS96 manual and user guide. Zürich: Hochschulverlag AG an der ETH; 1996.
28. Berendsen HJC, Grigera JR, Straatsma TP. The missing term in effective pair potentials. *J Phys Chem* 1987;91:6269–6271.
29. Fioroni M, Burger K, Mark A, Roccatano D. A new 2,2,2-trifluoroethanol model for molecular dynamics simulations. *J Phys Chem B* 2000;104:12347–12354.
30. Berendsen HJC, Postma JPM, van Gunsteren WF, Di Nola A, Haak JR. Molecular dynamics with coupling to an external bath. *J Chem Phys* 1984;81:3684–3690.
31. Jarvet J, Damberg P, Bodell K, Eriksson LEG, Graslund A. Reversible random coil to  $\beta$ -sheet transition and the early stage of aggregation of the A $\beta$ (12–28) fragment from the Alzheimer peptide. *J Am Chem Soc* 2000;122:4261–4268.
32. Jarvis RA, Patrick EA. Clustering using a similarity measure based on shared near neighbors. *IEEE Trans Comp* 1973;22:1025–1034.
33. Huang Z, Prusiner SB, Cohen FE. Scrapie prions: a three-dimensional model of an infectious fragment. *Fold Des* 1996;1:13–19.
34. Alonso D, DeArmond S, Cohen F, Daggett V. Mapping the early steps in the pH-induced conformational conversion of the prion protein. *Proc Natl Acad Sci USA* 2001;98:2985–2989.
35. Serpell LC, Blake CCF, Fraser PE. Molecular structure of a fibrillar Alzheimer's A $\beta$ -fragment. *Biochemistry* 2000;39:13269–13275.
36. Satheeshkumar K, Jayakumar R. Conformational polymorphism of the amyloidogenic peptide homologous to residues 113–127 of the prion protein. *Biophys J* 2003;85:473–483.
37. Jasanoff A, Fersht A. Quantitative determination of helical propensities from trifluoroethanol titration curves. *Biochemistry* 1994;33:2129–2135.
38. Lacroix E, Kortemme T, Lopez de la Paz M, Serrano L. The design of linear peptides that fold as monomeric  $\beta$ -sheet structures. *Curr Opin Struct Biol* 1999;9:487–493.
39. Booth DR, Sundet M, Bellotti V, Robinson CV, Hutchinson WL, Fraser PE, Hawkins PN, Dobson CM, Radford SE, Blake CCF, Pepys MB. Instability, unfolding and aggregation of human lysozyme variants underlying amyloid fibrillogenesis. *Nature* 1997;385:787–793.
40. Fandrich M, Fletcher MA, Dobson CM. Amyloid fibrils from muscle myoglobin. *Nature* 2001;410:165–166.
41. Lopez De La Paz M, Goldie K, Zurdo J, Lacroix E, Dobson C, Hoenger A, Serrano L. De novo designed peptide-based amyloid fibrils. *Proc Natl Acad Sci USA* 2002;99:16052–16057.
42. Kabsch W, Sander C. Dictionary of protein secondary structure: pattern recognition of hydrogen bonded and geometrical features. *Biopolymers* 1983;22:2577–2637.